Saturation of intervalence-band transitions in p-type semiconductors

R. B. James and D. L. Smith
California Institute of Technology, Pasadena, California 91125
(Received 15 October 1979)

We present a theory of the saturation of heavy-hole to light-hole band absorption in p-type semiconductors with the diamond or zinc-blende crystal structure by high-intensity light with a wavelength near 10 μm. The absorption coefficient is found to decrease with intensity in a manner closely approximated by an inhomogeneously broadened two-level model. For temperatures and hole concentrations where hole-phonon scattering dominates hole-impurity and hole-hole scattering, the saturation intensity is independent of the hole concentration. We calculate the saturation intensity as a function of excitation wavelength and temperature for p-Ge and p-GaAs. We find that the saturation intensity increases with photon energy and with temperature. The calculated results are compared with the available experimental data and good agreement is found.

I. INTRODUCTION

In many p-type semiconductors, direct free-hole transitions between the heavy- and light-hole bands are primarily responsible for the absorption of light with wavelengths near 10 μm. At high light intensities, absorption due to these transitions has been found to saturate in p-Ge (Refs. 1–4) and p-GaAs.[1] This saturation property allows a means of passively mode locking a CO_2 laser by inserting a slice of p-Ge or p-GaAs into the optical path of the cavity. Experiments have demonstrated that a CO_2 laser with p-Ge used as a saturable absorber can generate passively mode-locked pulses of subnanosecond duration.[5-7] In this paper, we present a theory of the saturation behavior of heavy-hole band to light-hole band transitions in p-type semiconductors at high light intensities. We present detailed numerical results for p-Ge and p-GaAs (the materials in which the effect has been experimentally observed). In a recent letter, we made a preliminary report of the results for p-Ge.[8]

In previous work, saturable absorption in p-type semiconductors has been described by modeling the valence bands as an ensemble of two-level systems whose level populations approach one another at high light intensities.[2-4,9] This two-level model predicts that the dependence of the absorption coefficient as a function of intensity is given by

$$\alpha(I,\omega)=\frac{\alpha_0(\omega)}{[1+I/I_s(\omega)]^{1/2}}\,, \tag{1}$$

where $\alpha_0(\omega)$ is the absorption coefficient at low intensity, and $I_s(\omega)$ is the saturation intensity. The behavior described in Eq. (1) was found to be reasonably well satisfied experimentally, and values of $I_s(\omega)$ were determined.[2-4] However, attempts to calculate $I_s(\omega)$ as a function of photon energy using the two-level model and a multistep cascade relaxation[9] gave results that disagree with experiment.[2] A theoretical discussion of saturable absorption in p-type Ge based on a spherical-parabolic-band model has also been presented.[10] However, the results of that discussion are qualitatively different than that of Eq. (1) and are in disagreement with experiment.

In this paper we present a theoretical analysis of the saturable absorption by considering the initial- and final-hole states in the optical transition to form a continuum with the valence-band structure determined by degenerate $\vec{k}\cdot\vec{p}$ perturbation theory.[11] Our calculated results are in close agreement with Eq. (1), and the values of $I_s(\omega)$ deduced from the calculation are in good agreement with experiment. We also determine the dependence of $I_s(\omega)$ on temperature. We present detailed results for p-Ge and p-GaAs; however, the theory should be applicable to other semiconductors with the zinc-blende crystal structure as well.

The paper is organized in the following way: in Sec. II we present our theoretical approach, in Sec. III we give the results for p-Ge, in Sec. IV we give the results for p-GaAs, and in Sec. V we summarize our conclusions. Calculational details are included in the Appendices.

II. THEORETICAL APPROACH

In semiconductors with the diamond or zinc-blende crystal structure, the valence-band maximum occurs at the zone center.[12] There are six bands (three sets of twofold degenerate bands) near the valence maximum. Four of the bands are degenerate at $k=0$ and the other two bands (degenerate) are split off to lower energy by the spin-orbit interaction. Away from the zone center, the bands degenerate at $k=0$ split into 2 twofold

degenerate pairs, the heavy-hole and light-hole bands. In p-type semiconductors free holes occur primarily in the heavy-hole band.

Light with a wavelength near 10 μm can induce transitions between the heavy-hole band and the light-hole band in p-type semiconductors. In Ge and GaAs (and several other materials), the spin-orbit splitting is greater than the photon energy for light with $\lambda \sim 10$ μm; thus transitions between the heavy-hole band and split-off band are not induced by light with this wavelength in these materials. The heavy- to light-hole transitions are the dominant absorption mechanism in p-Ge and p-GaAs.[13-16] For example, at $\lambda = 10.6$ μm and room temperature the intervalence-band absorption cross section in Ge is 6×10^{-16} cm^2.[15] The intervalence-band absorption cross section, estimated from Drude-Zener theory is about 10^{-17} cm^2, and the absorption coefficient from multiphonon absorption is about 0.013 cm^{-1}.[17] Thus, for hole concentrations in the 10^{15} cm^{-3} range intervalence-band absorption is 1 to 2 orders of magnitude greater than the other absorption processes.

Both energy and wave vector are conserved in the intervalence-band optical transitions. Thus, only holes in a narrow region of the heavy-hole band can directly participate in the absorption, and the absorption coefficient is governed by the population of these hole states. The optical transitions tend to deplete the population of the pertinent heavy-hole states. At low intensities, the heavy-hole states involved in the optical transition is maintained close to the equilibrium value by various scattering processes. However, as the intensity becomes large, scattering cannot maintain the equilibrium population of the pertinent heavy-hole states, and they become depleted. As a result the absorption saturates at high intensity. To determine the saturation characteristics of the intervalence-band transitions, it is necessary to set up rate equations for the hole distribution function in the heavy- and light-hole bands.

For the hole concentrations and temperatures at which most saturable absorption measurements have been performed (room temperature and $N_h \lesssim 5\times10^{15}$ cm^{-3}), hole-phonon scattering is the dominant relaxation mechanism. We consider only this scattering mechanism. The system can then be described by the Hamiltonian

$$H = H_0 + V + \gamma(t), \tag{2a}$$

where

$$H_0 = H_\epsilon + H_{ph} \tag{2b}$$

and

$$\gamma(t) = \frac{e}{mc}\vec{A}(t)\cdot\vec{P}. \tag{2c}$$

Here H_ϵ describes the free holes, H_{ph} describes the phonon system, V is the hole-phonon interaction, and $\gamma(t)$ describes the interaction of the holes with the electromagnetic field. The electromagnetic field is described by the vector potential $\vec{A}$; in the Coulomb gauge $\vec{A}$ satisfies the wave equation

$$\nabla^2\vec{A} - \frac{\epsilon_\infty}{c^2}\frac{\partial^2\vec{A}}{\partial t^2} = -\frac{4\pi}{c}\vec{J}, \tag{3}$$

where $\vec{J}$ is the current density induced by the intervalence-band transitions

$$\vec{J} = N_h\frac{e}{m}\,\mathrm{Tr}(\sigma\vec{P}'). \tag{4}$$

Here N_h is the hole density, σ is the one-hole density matrix, and $\vec{P}'$ is the off-diagonal (including only intervalence-band matrix elements) part of the hole momentum operator.

In Appendix A, we examine the time evolution of the density matrix σ. We find that σ is diagonal in wave vector and define

$$\langle b\vec{k}|\,\sigma\,|b'\vec{k}\rangle = \sigma_{bb'}(\vec{k}), \tag{5}$$

where $\vec{k}$ labels the wave vector, and b is the band index. The band index diagonal matrix elements of σ are determined by

$$\frac{d}{dt}\sigma_{bb}(\vec{k},t) = -\frac{i}{\hbar}[\gamma(\vec{k},t),\sigma(\vec{k},t)]_{bb} - \sum_{c\vec{k}'}[R_{b\vec{k}\to c\vec{k}'}\sigma_{bb}(\vec{k},t) - R_{c\vec{k}'\to b\vec{k}}\sigma_{cc}(\vec{k}',t)], \tag{6a}$$

and the off-diagonal elements are determined by

$$\frac{d}{dt}\sigma_{bb'}(\vec{k},t) = -\frac{i}{\hbar}[H_\epsilon(\vec{k}) + \gamma(\vec{k},t),\sigma(\vec{k},t)]_{bb'} - \frac{1}{T_2(\vec{k})}\sigma_{bb'}(\vec{k},t), \tag{6b}$$

where

$$\frac{2}{T_2(\vec{k})} = \sum_{c\vec{k}'}(R_{h\vec{k}\to c\vec{k}'} + R_{l\vec{k}\to c\vec{k}'}). \tag{6c}$$

Here $R_{a\vec{k}\to b\vec{k}'}$ is the rate at which a hole in band a with wave vector $\vec{k}$ is scattered into a state in band b with wave vector $\vec{k}'$, h (l) refers to the heavy- (light-) hole band, and $\gamma(\vec{k})$ and $H_\epsilon(\vec{k})$ are defined analogous to Eq. (5).

Using the equations for the time evolution of σ, the current density owing to intervalence-band transitions is found (details are found in Appendix B) to be determined by

$$\frac{d^2}{dt^2}\vec{J}(\vec{k})+\frac{2}{T_2(\vec{k})}\frac{d}{dt}\vec{J}(\vec{k})+\Omega^2(\vec{k})\vec{J}(\vec{k})$$
$$=N_h\frac{e^2}{\hbar^2m^2c}$$
$$\times\sum_{bc}f_b(\vec{k})[E_c(\vec{k})-E_b(\vec{k})][\vec{A}\cdot\vec{P}_{bc}(\vec{k})\vec{P}_{cb}(\vec{k})$$
$$+\vec{P}_{bc}\vec{A}\cdot\vec{P}_{cb}(\vec{k})]. \quad (7)$$

Here $E_b(\vec{k})$ is the energy of a hole in band b with wave vector $\vec{k}$, $\hbar\Omega(\vec{k})$ is $E_h(\vec{k})-E_l(\vec{k})$, we rename the diagonal elements of the hole density matrix $f_b(\vec{k})$, and $\vec{J}(\vec{k})$ is the part of $\vec{J}$ which includes only those terms in the trace with wave vector $\vec{k}$ ($\sum_{\vec{k}}\vec{J}(\vec{k})=\vec{J}$). Assuming both $\vec{A}$ and $\vec{J}(\vec{k})$ oscillate in time with angular frequency ω and that only terms with $\Omega(\vec{k})\sim\omega$ contribute, we have[18]

$$\vec{J}=N_h\frac{e^2}{3m^2c\hbar}\vec{A}\sum_{\vec{k}}[f_h(\vec{k})-f_l(\vec{k})]$$
$$\times\frac{|\vec{P}_{hl}(\vec{k})|^2}{[\Omega(\vec{k})-\omega]-i/T_2(\vec{k})}, \quad (8)$$

where the squared momentum matrix element $|\vec{P}_{hl}(\vec{k})|^2$ is to be summed over the two degenerate states in both the heavy- and light-hole bands. For a plane wave-vector potential

$$\vec{A}=\vec{A}_0e^{i(\vec{K}\cdot\vec{r}-\omega t)}, \quad (9)$$

the complex propagation constant is given by

$$K^2=\frac{\epsilon_\infty\omega^2}{c^2}\left(1+\frac{4\pi}{\epsilon_\infty\omega^2}\frac{N_he^2}{3m^2\hbar}\sum_{\vec{k}}[f_h(\vec{k})-f_l(\vec{k})]|\vec{P}_{hl}(\vec{k})|^2\frac{[\Omega(\vec{k})-\omega]+i/T_2(\vec{k})}{[\Omega(\vec{k})-\omega]^2+[1/T_2(\vec{k})]^2}\right). \quad (10)$$

Assuming that the second term in the parentheses of Eq. (10) is small compared to unity, the absorption coefficient is given by

$$\alpha(I,\omega)=2\,\mathrm{Im}(K)$$
$$=\frac{4\pi^2}{\sqrt{\epsilon_\infty}m^2\omega c}\frac{N_he^2}{3}\sum_{\vec{k}}[f_h(\vec{k})-f_l(\vec{k})]|\vec{P}_{hl}(\vec{k})|^2\frac{1/\hbar\pi T_2(\vec{k})}{[\Omega(\vec{k})-\omega]^2+[1/T_2(\vec{k})]^2}. \quad (11)$$

Equation (11) is the usual expression for the absorption coefficient except that a normalized Lorentzian replaces the usual energy conserving δ function. The intensity dependence of the absorption coefficient is contained in the distribution functions $f_h(\vec{k})$ and $f_l(\vec{k})$.

In order to determine the absorption coefficient, we must calculate the distribution functions for free holes in the heavy- and light-hole bands as a function of intensity. In the semiconductors of interest, the scattering rate for free holes occurs on a subpicosecond time scale. For a saturating laser operating with nanosecond pulse widths (the typical experimental situation), transient effects are damped out. Thus, we are interested in the steady-state values of the distribution functions. Using Eqs. (6a)–(6c) the steady-state distribution functions are found to solve (details are found in Appendix C) the rate equations

$$\beta(\vec{k})[f_h(\vec{k})-f_l(\vec{k})]=-\sum_{c\vec{k}'}[R_{h\vec{k}\to c\vec{k}'}f_h(\vec{k})$$
$$-R_{c\vec{k}'\to h\vec{k}}f_c(\vec{k}')], \quad (12a)$$

$$\beta(\vec{k})[f_h(\vec{k})-f_l(\vec{k})]=\sum_{c\vec{k}'}[R_{l\vec{k}\to c\vec{k}'}f_l(\vec{k})$$
$$-R_{c\vec{k}'\to l\vec{k}}f_c(\vec{k}')], \quad (12b)$$

where

$$\beta(\vec{k})=\frac{2\pi^2}{\sqrt{\epsilon_\infty}m^2\omega c}\frac{e^2I}{3\hbar\omega}|\vec{P}_{hl}(\vec{k})|^2$$
$$\times\frac{1/\pi\hbar T_2(\vec{k})}{[\Omega(\vec{k})-\omega]^2+[1/T_2(\vec{k})]^2}. \quad (12c)$$

These equations state that the rate of optical excitation out of (into) a given state is equal to the net rate of scattering into (out of) the state when steady state is attained. The left-hand sides of Eqs. (12a) and (12b) give the net rate of optical excitation out of a state with wave vector $\vec{k}$ in the heavy-hole band into a state with wave vector $\vec{k}$ in the light-hole band. The right-hand side of Eq. (12a) gives the net rate of scattering into the state with wave vector $\vec{k}$ in the heavy-hole band, and the right-hand side of Eq. (12b) gives the net rate of scattering out of the state with wave vector $\vec{k}$ in the light-hole band.

To calculate the absorption coefficient as a function of intensity, we first solve Eq. (12) for the distribution functions and then integrate Eq. (11). In solving Eq. (12), it is convenient to introduce the auxiliary functions defined by

$$\frac{1}{T_h(\vec{k})}=\sum_{c\vec{k}'}R_{h\vec{k}\to c\vec{k}'}, \quad (13a)$$

$$\frac{1}{T_l(\vec{k})}=\sum_{c\vec{k}'}R_{l\vec{k}\to c\vec{k}'}, \quad (13b)$$

$$F(\vec{k}) = \sum_{c\vec{k}'} R_{c\vec{k}' \to h\vec{k}} [f_c(\vec{k}') - f_c^e(\vec{k}')], \tag{13c}$$

and

$$G(\vec{k}) = \sum_{c\vec{k}'} R_{c\vec{k}' \to l\vec{k}} [f_c(\vec{k}') - f_c^e(\vec{k}')], \tag{13d}$$

where $f_c^e(\vec{k})$ is the equilibrium value for the distribution function. The function $F(\vec{k})$ is the difference in the feeding rate of free holes from the equilibrium feeding rate for the state with wave vector $\vec{k}$ in the heavy-hole band. The function $G(\vec{k})$ is analogously defined for the light-hole band. [Scattering into the light-hole band is small because of the small density of light-hole states. Thus the function $G(\vec{k})$ is less important than $F(\vec{k})$.] In terms of the auxiliary functions, the distribution functions can be written as

$$f_h(\vec{k}) = f_h^e(\vec{k}) - \frac{\beta(\vec{k}) T_h(\vec{k}) [f_h^e(\vec{k}) - f_l^e(\vec{k})]}{1 + \beta(\vec{k})[T_h(\vec{k}) + T_l(\vec{k})]} + \frac{F(\vec{k}) T_h(\vec{k}) + \beta(\vec{k}) T_h(\vec{k}) T_l(\vec{k}) [F(\vec{k}) + G(\vec{k})]}{1 + \beta(\vec{k})[T_h(\vec{k}) + T_l(\vec{k})]} \tag{14a}$$

and

$$f_l(\vec{k}) = f_l^e(\vec{k}) + \frac{\beta(\vec{k}) T_l(\vec{k}) [f_h^e(\vec{k}) - f_l^e(\vec{k})]}{1 + \beta(\vec{k})[T_h(\vec{k}) + T_l(\vec{k})]} + \frac{G(\vec{k}) T_l(\vec{k}) + \beta(\vec{k}) T_h(\vec{k}) T_l(\vec{k}) [F(\vec{k}) + G(\vec{k})]}{1 + \beta(\vec{k})[T_h(\vec{k}) + T_l(\vec{k})]} . \tag{14b}$$

The difference in occupation probabilities which appears in the expression for the absorption coefficient is given by

$$f_h(\vec{k}) - f_l(\vec{k}) = \frac{f_h^e(\vec{k}) - f_l^e(\vec{k})}{1 + \beta(\vec{k})[T_h(\vec{k}) + T_l(\vec{k})]} + \frac{T_h(\vec{k}) F(\vec{k}) - T_l(\vec{k}) G(\vec{k})}{1 + \beta(\vec{k})[T_h(\vec{k}) + T_l(\vec{k})]} . \tag{15}$$

The first term in Eq. (15) gives the population difference that would occur for the states at $\vec{k}$ if the populations of the states that feed those at $\vec{k}$ were given by their equilibrium values. The second term in Eq. (12) accounts for the change in the population of the states that feed those at $\vec{k}$. For those values of $\vec{k}$ which are important in the integral in Eq. (11), the first term in Eq. (15) is found to be significantly greater than the second.

Using Eq. (12) and the definition of the auxiliary functions, one can write equations which determine $F(\vec{k})$ and $G(\vec{k})$. If there is no angular dependence in the phonon scattering matrix elements which go into the scattering rates, the functions $F(\vec{k})$ and $G(\vec{k})$ depend on $E_h(\vec{k})$ and $E_l(\vec{k})$, respectively. Thus, one-dimensional (rather than three-dimensional) equations must be solved to determine these functions. Our treatment of these functions is included in Appendix D.

III. CALCULATION AND RESULTS FOR *p*-Ge

In order to calculate the difference in occupation probabilities for the heavy- and light-hole bands, it is necessary to know the free-hole scattering rates. We consider the region of temperature and impurity densities for which hole-phonon scattering is the dominant scattering mechanism. Optical-phonon scattering is the dominant energy relaxation mechanism. The optical-phonon spectrum is relatively flat for small k with an average energy of 0.037 eV. For the small k region in which we are interested, the acoustic phonon energy is quite small, and we neglect it. Although acoustic phonon scattering does not contribute significantly to energy relaxation, it can change the wave vector of the hole. The valence bands of Ge are rather anisotropic and an acoustic phonon scattering event can take a hole from a region in which $\beta(\vec{k})$ is small to one in which it is large. Thus, although acoustic phonon scattering is less important than optical phonon scattering in determining the distribution functions, it is not negligible because of the anisotropy of the valence bands. We take the scattering rates to be given by[19]

$$R_{a\vec{k} \to b\vec{k}'} = \frac{2\pi}{\hbar} |M_{op}^{+}|^2 (E_a(\vec{k}) - E_b(\vec{k}') + \hbar\omega_0) + \frac{2\pi}{\hbar} |M_{op}^{-}|^2 \delta(E_a(\vec{k}) - E_b(\vec{k}') - \hbar\omega_0) + \frac{2\pi}{\hbar} |M_{ac}|^2 \delta(E_a(\vec{k}) - E_b(\vec{k}')), \tag{16a}$$

where

$$|M_{op}^{+}|^2 = \frac{E_{op}^2 \hbar\omega_0}{2V\rho u_l^2} (N_q + 1), \tag{16b}$$

$$|M_{op}^{-}|^2 = \frac{E_{op}^2 \hbar\omega_0}{2V\rho u_l^2} N_q , \tag{16c}$$

and

$$|M_{ac}|^2 = \frac{E_{ac}^2 k_B T}{2V\rho u_l^2} . \tag{16d}$$

Here $|M_{op}^{+}|^2$ is the squared matrix element for optical phonon emission, $|M_{op}^{-}|^2$ is the squared matrix element for optical phonon absorption, and $|M_{ac}|^2$ is the squared acoustic phonon scattering matrix element (summed over both absorption and emission processes). In Eq. (16), E_{op} (E_{ac}) is the deformation potential for optical (acoustical) phonon scattering, $\hbar\omega_0$ is the zone-center optical phonon energy, ρ is the density, u_l is the longitudinal sound velocity, N_q is the optical phonon Bose factor, and V is the sample volume. Following Ref. 19, we have neglected angular dependence in the phonon scattering matrix element and taken the scattering rates to be the same for the heavy- and light-hole bands. The numerical value for the constants appearing in the squared matrix elements were taken from the mobility fits of Ref. 20; they are listed in Table I. The scattering times $T_2(\vec{k})$, $T_h(\vec{k})$, and $T_l(\vec{k})$ are computed from Eqs. (6c), (13a), and (13b) using these scattering rates. Optical phonon scattering (primarily emission) dominates in the results for $T_2(\vec{k})$ and $T_l(\vec{k})$ for the states of interest. For $T_h(\vec{k})$ in the resonant region, optical phonon emission is typically not possible and acoustic phonon scattering makes a significant contribution to $T_h(\vec{k})$.

The free-hole energies $E_h(\vec{k})$ and $E_l(\vec{k})$ and the momentum matrix elements $|\vec{P}_{hl}(\vec{k})|^2$ are determined by degenerate $\vec{k}\cdot\vec{p}$ perturbation theory.[11] The cyclotron resonance parameters of Hensel and Suzuki[21] are used.

TABLE I. Valence-band deformation potentials used in the calculation of phonon scattering rates.

	E_{ac} (eV)	E_{op} (eV)
Ge	3.5 [a]	6.8 [a]
GaAs	3.6 [b]	6.5 [b]

[a]Reference 20.
[b]Reference 23.

A. First approximation for $f_h(\vec{k}) - f_l(\vec{k})$

As a first approximation for the population difference $f_h(\vec{k}) - f_l(\vec{k})$, we neglect the auxiliary functions $F(\vec{k})$ and $G(\vec{k})$ and include only the first term in Eq. (15). This approximation is equivalent to assuming that the rate at which free holes are scattered into the states involved in the optical transition is given by the equilibrium value. For optical phonon scattering, the energy of the initial-hole state in the scattering event differs from that of the final-hole state by the optical phonon energy. As a result, hole states that can scatter into a resonant optical transition region by optical phonon scattering are, for the most part, themselves out of the resonant region. Thus, the population of these states is not directly depleted by the optical transitions. The population of these states is indirectly depleted by the optical transition because there is a decrease in the feeding rate of these states owing to the decrease in population of hole states in the resonant region. However, this decreased feeding from the resonant region is partially compensated for by an increased feeding from the rerouting of optically excited holes.

For acoustic phonon scattering, the energy of the initial-hole state in the scattering event is essentially the same as that of the final-hole state. As a result, hole states that can scatter into a resonant optical transition region by acoustic phonon scattering are, for the most part, in the resonant region themselves. Thus, the population of these states is directly depleted by the optical transitions. Including only the first term in Eq. (15), therefore, overestimates the importance of acoustic phonon scattering. At this level of approximation, it is better to ignore acoustic phonon scattering. We will see that this first approximation for $f_h(\vec{k}) - f_l(\vec{k})$ ignoring acoustic phonon scattering produces results close to that of our more complete calculation.

Using only the first term in Eq. (15) to determine the population difference, the absorption coefficient becomes

$$\alpha^1(I,\omega) = \frac{4\pi^2}{\sqrt{\epsilon_\infty}\, m^2\omega c}\frac{N_h e^2}{3}\sum_{\vec{k}}\left[f_h^e(\vec{k}) - f_l^e(\vec{k})\right]|\vec{P}_{hl}(\vec{k})|^2\,\frac{1/[\hbar\pi T_2(\vec{k})]}{[\Omega(\vec{k})-\omega]^2 + [1/T_2(\vec{k})]^2[1 + I/I(\vec{k})]}\,, \tag{17a}$$

where

$$I(k) = \frac{3\hbar^2 c\sqrt{\epsilon_\infty}\, m^2\omega^2}{[T_h(\vec{k}) + T_l(\vec{k})]T_2(\vec{k})2\pi e^2|\vec{P}_{hl}(\vec{k})|^2}\,. \tag{17b}$$

Transforming to an integration over surfaces of constant $\Omega(\vec{k})$, and assuming that the power-broadened Lorentzian is sharply peaked, Eq. (17a) can be written as

$$\alpha^1(I,\omega) = \frac{4\pi^2}{\sqrt{\epsilon_\infty}\, m^2\omega c}\frac{N_h e^2}{3\hbar}\left(\frac{1}{2\pi}\right)^3\int_{\Omega(\vec{k})=\omega}\frac{ds}{|\nabla_{\vec{k}}\Omega(\vec{k})|}\,\frac{|\vec{P}_{hl}(\vec{k})|^2[f_h^e(\vec{k}) - f_l^e(\vec{k})]}{[1 + I/I(\vec{k})]^{1/2}}\,. \tag{18}$$

Here the integral is over a surface of constant $\Omega(\vec{k})$. Integrating Eq. (18) numerically, we find that the absorption coefficient satisfies Eq. (1) to high accuracy. Indeed, if $l(\vec{k})$ were independent of $\vec{k}$ over the region of the surface integral, Eq. (18) would reduce to Eq. (1) exactly.

For hole densities and temperatures such that hole-phonon scattering dominates the hole-impurity and hole-hole scattering events, values of $I_s(\omega)$ deduced from Eq. (18) are independent of the hole density. Experimentally $I_s(\omega)$ has been found to be independent of hole density for densities less than 4×10^{15} cm^{-3} at room temperature.[1]

B. Higher-order approximation for $f_h(\vec{k}) - f_l(\vec{k})$

The auxiliary functions $F(\vec{k})$ and $G(\vec{k})$ are computed numerically as discussed in Appendix D. The distribution function computed from these auxiliary functions for $\vec{k}$ in the [111] and [100] directions together with their equilibrium values are shown in Fig. 1. The dominant dip in the heavy-hole distribution function and corresponding peak in the light-hole distribution function is due to direct optical transitions. Additional dips in the heavy-hole distribution function occur because of the discrete energy of the optical phonons. The increase in the heavy-hole distribution compared to the equilibrium value at large values of k is due to scattering of the photoexcited holes in the light-hole band into the heavy-hole band.

The absorption coefficient is calculated numerically. The calculated result for $\lambda = 10.6$ μm and $T = 295$ °K is compared with the expression in Eq. (1) in Fig. 2. The value of I_s used in Eq. (1) was determined by fitting the calculated result for $\alpha(I, \omega)$. The numerical results could be fit to an accuracy of about 5% for intensities less than 25 times I_s. (This is the range of intensities which has been most frequently explored experimentally.) If only the first term in Eq. (15) is retained, the calculated $\alpha(I, \omega)$ has almost exactly the form of Eq. (1). The second term in Eq. (15) is smaller than the first and leads to the small deviations seen in Fig. 2.

Measurements of the saturable absorption in p-type Ge have been interpreted in terms of the inhomogeneously broadened two-level model which produces Eq. (1), and the values of $I_s(\omega)$ have been reported. In Fig. 3, we compare measured values of $I_s(\omega)$ at room temperature as a function of photon energy with our theoretical values. The theoretical values of $I_s(\omega)$ are determined by fitting the expression in Eq. (1) to the calculated results for $\alpha(I, \omega)$ for intensities between zero and 100 MW/cm^2. In the range of photon energies considered, $I_s(\omega)$ was found to increase monotonically with photon energy. There

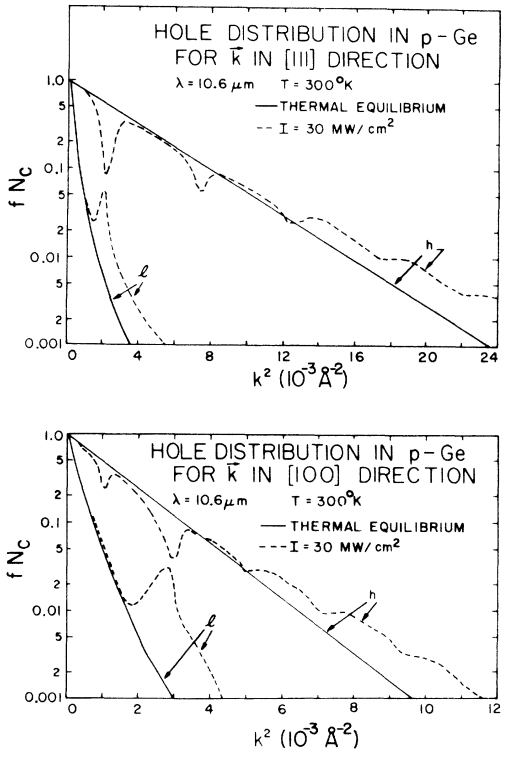

FIG. 1. Calculated hole distribution functions in p-Ge as a function of k^2 for $\vec{k}$ in the [111] and [100] directions. The calculations were performed for $\lambda = 10.6$ μm, $T = 300$ °K, and $I = 30$ MW/cm^2. The equilibrium distribution functions are shown for comparison. N_c is the effective density of states.

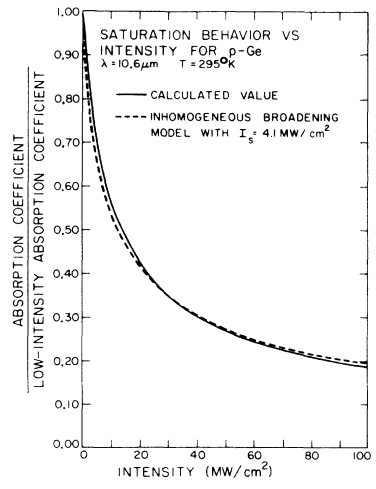

FIG. 2. Calculated absorption coefficient normalized to its low intensity value as a function of intensity for p-Ge. The calculations were performed for $\lambda = 10.6$ μm and $T = 295$ °K. The inhomogeneously broadened two-level model result with $I_s = 4.1$ MW/cm^2 is also shown.

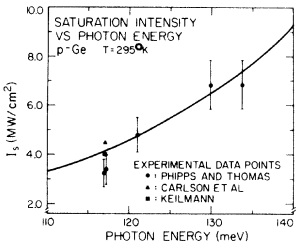

FIG. 3. Calculated saturation intensity as a function of photon energy for p-Ge at 295 °K. The experimental results are from Refs. 2–4. Error bars are only given in Ref. 2.

is good agreement between theory and experiment. There are no adjustable parameters in the theory.

The calculated results shown in Fig. 3 were attained using the higher-order approximation for $f_h(\vec{k}) - f_l(\vec{k})$. The results for the first-order approximation are qualitatively similar to those of the more complete calculation; the numerical values of the two calculations differ by an approximately constant factor. At $\lambda = 10.6\ \mu$m and $T = 295$ °K, the more complete calculation gives a value of I_s of 4.1 MW/cm^2, the first-order calculation including acoustic phonon scattering gives a result of 5.8 MW/cm^2, and the first-order calculation neglecting acoustic phonon scattering gives a result of 3.5 MW/cm^2. Thus the first-order calculation neglecting acoustic phonon scattering is within about 15% of the more complete calculation. This result is interesting because the first-order calculation is much easier and less expensive to perform than the more complete calculation.

The increase in $I_s(\omega)$ with increasing ω is due both to the behavior of the scattering rates and the optical matrix elements. The relative contribution of the scattering rates and the optical matrix elements can be most easily seen in the first-order calculation. At this level of approximation, $I_s(\omega)$ is given by a weighted average of $l(\vec{k})$ [see Eq. (18)]. The values of $l(\vec{k})$ are proportional to ω^2, $T_2^{-1}(\vec{k})$, $[T_h(\vec{k}) + T_l(\vec{k})]^{-1}$, and $|\vec{P}_{hl}(\vec{k})|^{-2}$. In Fig. 4, the variation of these factors is illustrated as a function of photon energy for $\vec{k}$ in the [100] and [111] directions.

Since the usefulness of p-Ge as a saturable absorber in CO_2 laser systems is determined by its saturation characteristics, it is of interest to be able to control the saturation behavior. Since optical phonon scattering is the dominant relaxation mechanism, and the optical phonon occupation is temperature dependent, it is clear that $I_s(\omega)$ will depend on temperature. In Fig. 5, we present the results of a calculation of the temperature

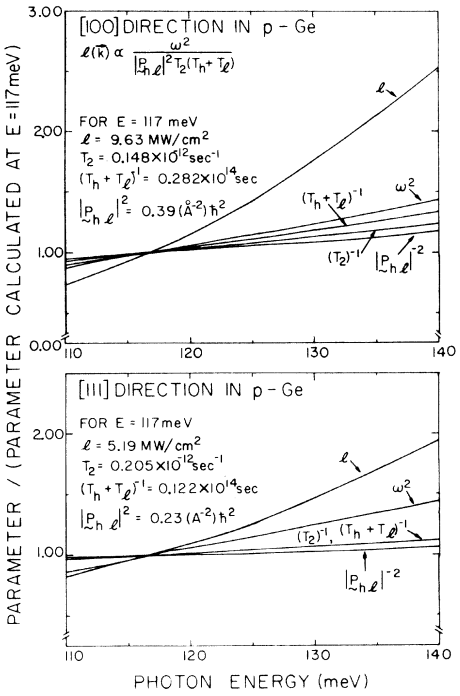

FIG. 4. Variation of the factors which contribute to the photon energy dependence of $I_s(\omega)$ in our first approximation for the absorption coefficient in p-Ge. The values of the factors are normalized to their value at $\hbar\omega = 117$ meV ($\lambda = 10.6\ \mu$m). The factors were computed for $T = 295$ °K.

dependence of $I_s(\omega)$ in p-Ge for light with a wavelength of 10.6 μm. $I_s(\omega)$ increases monotonically with temperature. This increase is due to the increased rate of phonon scattering at higher temperatures. Because of the rather strong dependence of $I_s(\omega)$ on temperature, it should be possible to tune the saturation behavior of p-Ge with temperature.

IV. CALCULATION AND RESULTS FOR p-GaAs

The dependence of the absorption coefficient on intensity in p-GaAs can be described by the same theory as in p-Ge. We use the cyclotron reso-

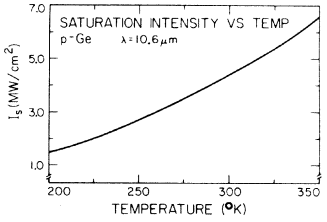

FIG. 5. Calculated saturation intensity as a function of temperature for p-Ge and light with a wavelength of 10.6 μm.

nance parameters of Lawaetz[22] to determine the GaAs valence-band structure. (We neglect the small terms linear in k which appear in the $\vec{k}\cdot\vec{p}$ perturbation theory for zinc-blende cyrstals.) Hole-phonon scattering is described as in Ge; the deformation potential parameters are taken from Ref. 23 and are listed in Table I. We neglect the small splitting between the zone-center LO and TO phonons and take an average optical phonon energy of 34.3 meV. The input parameters that we use for GaAs are not as accurately known as those for Ge.

Our calculations of the intensity dependence of the absorption coefficient give a result that is numerically close to the inhomogeneously broadened two-level model result of Eq. (1).[24] In Fig. 6, we compare the calculated result for $\lambda = 10.6$ μm and $T = 295$ °K with Eq. (1). As for Ge, the small difference between the calculated result and inhomogeneously broadened two-level model result comes from the second term in Eq. (15).

In Fig. 7, we show the theoretical results for $I_s(\omega)$ as a function of photon energy at room temperature. The theoretical results are determined by fitting the expression in Eq. (1) to the calculated results for $\alpha(I, \omega)$ for intensities between zero and 100 MW/cm^2. The results for $I_s(\omega)$ are qualitatively similar to those for Ge except that $I_s(\omega)$ is uniformly larger in GaAs than in Ge. The values of $I_s(\omega)$ are larger in GaAs than in Ge primarily because the hole-phonon scattering times are shorter in GaAs. The scattering times are shorter in GaAs because the heavy-hole effective mass is larger in GaAs, and as a result the density of final scattering states is larger in GaAs.

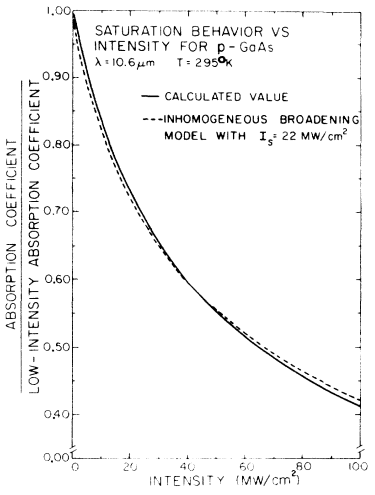

FIG. 6. Calculated absorption coefficient normalized to its low-intensity value as a function of intensity for p-GaAs. The calculations were performed for $\lambda = 10.6$ μm and $T = 295$ °K. The inhomogeneously broadened two-level model result with $I_s = 22$ MW/cm^2 is also shown.

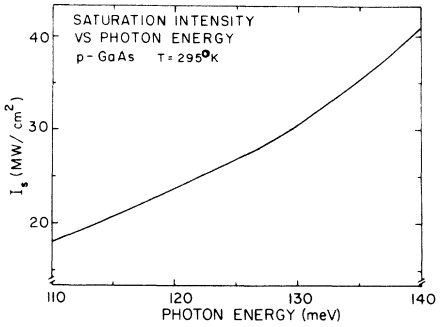

FIG. 7. Calculated saturation intensity as a function of photon energy for p-GaAs at 295 °K.

Saturation of intervalence-band absorption in p-GaAs has been observed in one experiment in p-GaAs.[1] A saturation intensity of $I_s = 20 \pm 5$ MW/cm^2 at $\lambda = 10.6$ μm and room temperature was reported. However, these measurements were performed over a relatively small range of incident intensities and were interpreted in terms of a homogeneously (rather than an inhomogeneously) broadened two-level model. If the results had been interpreted in terms of the inhomogeneously broadened two-level model (which we believe would have been more correct), a smaller value of I_s would most likely have been attained.

In Fig. 8, we present the results of a calculation of the temperature dependence of the saturation intensity at $\lambda = 10.6$ μm in p-GaAs. As for Ge, I_s is an increasing function of temperature owing to the increased phonon scattering rates at higher temperature.

V. SUMMARY AND CONCLUSIONS

We have presented a theory of saturation of heavy- to light-hole band transitions in p-type semiconductors with the diamond or zinc-blende crystal structure. Detailed calculations have

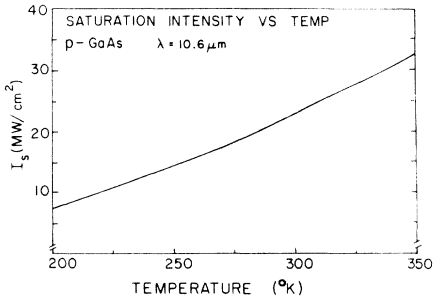

FIG. 8. Calculated saturation intensity as a function of temperature for p-GaAs and light with a wavelength of 10.6 μm.

been presented for p-type Ge and GaAs. We found that the intensity dependence of the absorption coefficient is closely approximated by an inhomogeneously broadened two-level model. For the temperature and concentration range where hole-phonon scattering dominates hole-impurity and hole-hole scattering, I_s is found to be independent of the hole density. This behavior is consistent with experimental results. The dependence of the saturation intensity on photon energy has been computed and compared with available experimental results. Good agreement between theory and experiment was found. We have predicted the dependence of the saturation intensity on temperature.

ACKNOWLEDGMENTS

The authors thank R. N. Silver and T. C. McGill for many useful discussions. We thank P. G. James, G. C. Osbourn, and M. S. Daw for assistance with the numerical calculations. We gratefully acknowledge the support of the Air Force Office of Scientific Research under Grant No. AFOSR-77-3216. One of us (D. L. S.) acknowledges support from the Alfred P. Sloan Foundation.

APPENDIX A: FREE-HOLE DENSITY MATRIX

In this appendix we outline the derivation of Eqs. (6a)–(6c) for the hole density matrix. We consider the low-hole density limit and take the Hamiltonian to be given by Eq. (2). The density matrix $\rho(t)$ satisfies

$$\frac{d\rho}{dt}=\frac{-i}{\hbar}[H,\rho]\,. \tag{A1}$$

We assume that ρ can be approximated by

$$\rho(t)\approx\sigma(t)P_L\,, \tag{A2}$$

where $\sigma(t)$ is the free-hole density matrix, and P_L describes the lattice in thermal equilibrium. Using standard approximations,[25] one finds

$$\frac{d\sigma_I(t)}{dt}\approx\frac{-i}{\hbar}[\gamma_I(t),\sigma_I(t)] -\frac{1}{\hbar^2}\int_0^\infty dt'\,\mathrm{Tr}_L[V_I(t),[V_I(t'),\sigma_I(t)P_L]]. \tag{A3}$$

Here the subscript I signifies that an operator is in the interaction representation, and Tr_L signifies a trace over lattice modes.

From Eq. (A3), one can see that $\sigma(t)$ is diagonal in wave vector. Prior to laser excitation, $\sigma(t)$ has the equilibrium value which is diagonal in wave vector. Taking matrix elements of Eq. (A3), we see that the time derivative of any matrix element of $d\sigma_I(t)/dt$ which is off-diagonal in $\vec{k}$ is equal to a sum of terms, all of which are proportional to a matrix element of $\sigma_I(t)$, which is off-diagonal in $\vec{k}$. Thus when the equation is integrated in time, all off-diagonal in $\vec{k}$ matrix elements of $\sigma_I(t)$ vanish. This result is to be expected since the electromagnetic field leads to transitions between states with the same wave vector. Taking matrix elements of Eq. (A3), dropping nonresonant terms and returning to the Schrödinger representation gives Eq. (6).

APPENDIX B: EQUATIONS OF MOTION FOR $\vec{J}(\vec{k})$

In this appendix we derive Eq. (7). Multiplying Eq. (6b) by $\vec{P}'$, taking the time derivative and tracing over bands gives

$$\frac{d^2}{dt^2}\mathrm{Tr}_b[\sigma(\vec{k},t)\vec{P}']+\frac{1}{T_2(\vec{k})}\frac{d}{dt}\mathrm{Tr}_b[\sigma(\vec{k},t)\vec{P}']=-\frac{i}{\hbar}\mathrm{Tr}_b\left(\frac{d\sigma(\vec{k},t)}{dt}[\vec{P}',H_\epsilon]\right). \tag{B1}$$

We have used the facts that σ, $\vec{P}'$, γ, and H_ϵ are all diagonal in $\vec{k}$ and hence can be cyclically permuted in the trace on bands and that $[\vec{P}',\gamma]$ vanishes. Using Eq. (6b), we can write

$$\frac{1}{\hbar}\mathrm{Tr}_b\left(\frac{d\sigma(\vec{k},t)}{dt}[\vec{P}',H_\epsilon]\right)=-\frac{i}{\hbar^2}\mathrm{Tr}_b\{\sigma(\vec{k},t)[(H_\epsilon+\gamma),[H_\epsilon,\vec{P}']]\}-\frac{i}{T_2(\vec{k})}\frac{d}{dt}\mathrm{Tr}_b[\sigma(\vec{k},t)\vec{P}'] -\frac{i}{[T_2(\vec{k})]^2}\mathrm{Tr}_b[\sigma(\vec{k},t)\vec{P}']\,. \tag{B2}$$

Thus Eq. (B1) becomes

$$\frac{d^2}{dt^2}\mathrm{Tr}_b[\sigma(\vec{k},t)\vec{P}']+\frac{2}{T_2(\vec{k})}\frac{d}{dt}\mathrm{Tr}_b[\sigma(\vec{k},t)\vec{P}']+\left(\frac{1}{T_2(\vec{k})}\right)^2\mathrm{Tr}_b[\sigma(\vec{k},t)\vec{P}']=-\frac{1}{\hbar^2}\mathrm{Tr}_b\{\sigma(\vec{k},t)[(H_\epsilon+\gamma),[H_\epsilon,\vec{P}']]\}\,. \tag{B3}$$

Evaluating the trace on the right-hand side, multiplying by $(N_h e/m)$, and neglecting $[1/T_2(\vec{k})]^2$ compared with $[\Omega(\vec{k})]^2$ gives Eq. (7).

APPENDIX C: EQUATIONS OF MOTION FOR THE DISTRIBUTION FUNCTIONS

In this appendix we derive the equations for the distribution functions $f_h(\vec{k})$ and $f_l(\vec{k})$. Multiplying Eq. (6b) by $(N_h e\vec{P}'/m)$ and taking the trace over bands gives

$$i\frac{d}{dt}\vec{J}(\vec{k})+\frac{i}{T_2(\vec{k})}\vec{J}(\vec{k})=\frac{N_h e}{m}\Omega(\vec{k})\sum_{\substack{b\ \text{in}\ h\\ b'\ \text{in}\ l}}[\sigma_{bb'}(\vec{k},t)\vec{P}_{b'b}(\vec{k})-\sigma_{b'b}(\vec{k},t)\vec{P}_{bb'}(\vec{k})]. \tag{C1}$$

Using Eq. (C1) and neglecting $[1/T_2(\vec{k})]$ compared with ω, Eq. (6a) can be written as (with b in the heavy-hole band)

$$\frac{df_h(\vec{k},t)}{dt}=-\frac{1}{2N_h c\hbar\Omega(\vec{k})}\left(\frac{d}{dt}\vec{J}(\vec{k})\cdot\vec{A}\right)-\sum_{c\vec{k}'}[R_{h\vec{k}\to c\vec{k}'}f_h(\vec{k},t)-R_{c\vec{k}'\to h\vec{k}}f_c(\vec{k}',t)]. \tag{C2}$$

With b in the light-hole band, Eq. (6a) can be written as

$$\frac{df_l(\vec{k},t)}{dt}=\frac{1}{2N_h c\hbar\Omega(\vec{k})}\left(\frac{d}{dt}\vec{J}(\vec{k})\cdot\vec{A}\right)-\sum_{c\vec{k}'}[R_{l\vec{k}\to c\vec{k}'}f_l(\vec{k},t)-R_{c\vec{k}'\to l\vec{k}}f_c(\vec{k}',t)]. \tag{C3}$$

Assuming $\vec{J}(\vec{k})$ and $\vec{A}$ have sinusoidal time dependence and averaging over many cycles, one gets the steady-state rate equations of Eq. (12).

APPENDIX D: AUXILIARY FUNCTIONS $F(\vec{k})$ AND $G(\vec{k})$

In this appendix we describe our treatment of the auxiliary functions $F(\vec{k})$ and $G(\vec{k})$. From the definition of these functions, we see that when the phonon scattering matrix elements are approximated as independent of the scattering angle, $F(\vec{k})$ depends on $E_h(\vec{k})$, and $G(\vec{k})$ depends on $E_l(\vec{k})$. Using the definitions of $F(\vec{k})$ and $G(\vec{k})$ and Eqs. (12a)–(12c) for the distribution functions, $F(E_h(\vec{k}))$ is seen to be determined by

$$\begin{aligned}F(E_h(\vec{k}))=&\sum_{\vec{k}'}[-R_{h\vec{k}'\to h\vec{k}}T_h(\vec{k}')+R_{l\vec{k}'\to h\vec{k}}T_l(\vec{k}')]\{[f_h^e(\vec{k}')-f_l^e(\vec{k}')]+F(E_h(\vec{k}'))T_h(\vec{k}')\\&-G(E_l(\vec{k}'))T_l(\vec{k}')\}\frac{\beta(\vec{k}')}{\beta(\vec{k}')[T_h(\vec{k}')+T_l(\vec{k}')]+1}\\&+\sum_{\vec{k}'}R_{h\vec{k}'\to h\vec{k}}F(E_h(\vec{k}'))T_h(\vec{k}')+\sum_{\vec{k}'}R_{l\vec{k}'\to h\vec{k}}G(E_l(\vec{k}))T_l(\vec{k}'),\end{aligned} \tag{D1}$$

and $G(E_l(\vec{k}))$ is determined by a similar equation where $(h\vec{k})$ in the scattering rates is replaced by $(l\vec{k})$. The function $G(\vec{k})$ describes the increased (from the equilibrium value) scattering into the light-hole band states. Because of the small density of light-hole band states, the magnitude of this function is much smaller than that of $F(\vec{k})$. In addition $T_h(\vec{k})$ is much greater than $T_l(\vec{k})$. Thus in Eq. (D1), we neglect $T_l(\vec{k})G(\vec{k})$ compared with $T_h(\vec{k})F(\vec{k})$. We have explicitly checked the self-consistency of this approximation at the end of the calculation.

Equation (D1) is an inhomogeneous, linear integral equation. Because of the energy conserving δ functions in the phonon scattering rates, it reduces to algebraic equations relating $F(E_h(\vec{k}))$ at different values of $E_h(\vec{k})$. The term proportional to $R_{l\vec{k}'\to h\vec{k}}F(E_h(\vec{k}'))$, however, is responsible for coupling the equation for $F(E_h(\vec{k}))$ to those for all other values of $E_h(\vec{k}')$. [In other terms, the equation for $F(E_h(\vec{k}))$ is only coupled to those for $F(E_h(\vec{k})+\hbar\omega_0)$ and $F(E_h(\vec{k})-\hbar\omega_0)$]. To overcome this difficulty, we approximate the first term on the right-hand side of Eq. (D1), which can be written as

$$\sum_{\vec{k}'}[-R_{h\vec{k}'\to h\vec{k}}T_h(\vec{k}')+R_{l\vec{k}'\to h\vec{k}}T_l(\vec{k}')]\times\beta(\vec{k}')[f_h(\vec{k}')-f_l(\vec{k}')],$$

by

$$X\sum_{\vec{k}'}[-R_{h\vec{k}'\to h\vec{k}}T_h(\vec{k}')+R_{l\vec{k}'\to h\vec{k}}T_l(\vec{k}')]\times\beta(\vec{k}')[f_h(\vec{k}')-f_l(\vec{k}')]^1, \tag{D2}$$

where $[f_h(\vec{k}')-f_l(\vec{k}')]^1$ is the first approximation to $f_h(\vec{k}')-f_l(\vec{k}')$; that is, the first term in Eq. (15). Here X is a function of $\hbar\omega$, T, and I, but is as-

sumed independent of $E_h(k)$. We determine X by requiring

$$\sum_{\vec{k}'}\beta(\vec{k}')[f_h(\vec{k}')-f_l(\vec{k}')] = X\sum_{\vec{k}'}\beta(\vec{k}')[f_h(\vec{k}')-f_l(\vec{k}')]^1 . \quad \text{(D3)}$$

Since scattering to the light-hole band is much slower than scattering to the heavy-hole band (owing to the small density of states in the light-hole band);

$$\sum_{\vec{k}} R_{h\vec{k}'\to h\vec{k}}T_h(\vec{k}') \approx \sum_{\vec{k}} R_{l\vec{k}'\to h\vec{k}}T_l(\vec{k}') \approx 1 . \quad \text{(D4)}$$

Thus Eq. (D3) assures that the integral of the positive and negative parts of Eq. (D2) are separately satisfied. We solve the equation

$$F(E_h(\vec{k})) = X\sum_{\vec{k}'}[-R_{h\vec{k}'\to h\vec{k}}T_h(\vec{k}')+R_{l\vec{k}'\to h\vec{k}}T_l(\vec{k}')] \times\beta(\vec{k}')[f_h(\vec{k}')-f_l(\vec{k}')]^1 + \sum_{\vec{k}'}R_{h\vec{k}'\to h\vec{k}}F(E_h(\vec{k}'))T_h(\vec{k}') , \quad \text{(D5)}$$

which is a series of inhomogeneous linear algebraic equations. We truncate the series for $E_h(\vec{k}) > 400$ meV. [$F(E_h(\vec{k}))$ is negligible for these high energies.] We first find the solution for $X=1$. Calling the result of this calculation F', F is given by XF'. We determine X from Eq. (D3) which reduces to

$$X = 1+\frac{X\left[\int_{\Omega(\vec{k})=\omega}\frac{ds\,|\vec{P}_{hl}(\vec{k})|^2T_h(k)F^1(E_h(\vec{k}))}{|\nabla_{\vec{k}}\Omega(\vec{k})|[1+I/I(\vec{k})]^{1/2}}\right]}{\left[\int_{\Omega(\vec{k})=\omega}\frac{ds[f_h^e(\vec{k})-f_l^e(\vec{k})]\,|\vec{P}_{hl}(\vec{k})|^2}{|\nabla_{\vec{k}}\Omega(\vec{k})|[1+I/I(\vec{k})]^{1/2}}\right]} . \quad \text{(D6)}$$

In order to limit the numerical expense, we approximate the surface integrals in Eq. (D6) using the four-point prescription suggested by Kane.[11]

From Eqs. (11) and (D3), we see that the function X relates the absorption coefficient calculated in the first approximation to the result of the more complete calculation by

$$\alpha(I,\omega) = X\alpha^1(I,\omega) , \quad \text{(D7)}$$

where $\alpha^1(I,\omega)$ is given by Eq. (18).

[1]A. F. Gibson, C. A. Rosito, C. A. Raffo, and M. F. Kimmitt, Appl. Phys. Lett. 21, 356 (1972).
[2]C. R. Phipps, Jr. and S. J. Thomas, Opt. Lett. 1, 93 (1977).
[3]R. L. Carlson, M. D. Montgomery, J. S. Ladish, and C. M. Lockhart, IEEE J. Quantum Electron. 13, 35D (1977).
[4]F. Keilmann, IEEE J. Quantum Electron. 12, 592 (1976).
[5]A. J. Alcock and A. C. Walker, Appl. Phys. Lett. 25, 299 (1974).
[6]B. J. Feldman and J. F. Figueria, Appl. Phys. Lett. 25, 301 (1974).
[7]A. F. Gibson, M. F. Kimmitt, and B. Norris, Appl. Phys. Lett. 24, 306 (1974).
[8]R. B. James and D. L. Smith, Phys. Rev. Lett. 42, 1495 (1979).
[9]M. Sargent III, Opt. Commun. 20, 298 (1977).
[10]V. L. Komolov, I. D. Yaroshetskii, and I. N. Yassievich, Fiz. Tekh. Poluprovodn. 11, 85 (1977) [Sov. Phys. Semicond. 11, 48 (1977)].
[11]E. O. Kane, J. Phys. Chem. Solids 1, 82 (1956).
[12]We neglect the small terms linear in k which appear in the $\vec{k}\cdot\vec{p}$ perturbation theory for zinc-blende crystals.
[13]H. B. Briggs and R. C. Fletcher, Phys. Rev. 91, 1342 (1953).
[14]A. H. Kahn, Phys. Rev. 97, 1647 (1955).
[15]W. Kaiser, R. J. Collins, and H. Y. Fan, Phys. Rev. 91, 1342 (1953).
[16]R. Braunstein, J. Phys. Chem. Solids 8, 280 (1959).
[17]A. J. Bishop and A. F. Gibson, Appl. Opt. 12, 2549 (1973).
[18]We neglect off-diagonal terms that can appear in the nonlinear susceptibility tensor for polarized light and we average over polarizations. That is, we consider the case of unpolarized light.
[19]E. Conwell, J. Phys. Chem. Solids 8, 236 (1959).
[20]D. M. Brown and R. Bray, Phys. Rev. 127, 1593 (1962).
[21]J. C. Hensel and K. Suzuki, Phys. Rev. B 9, 4219 (1974).
[22]P. Lawaetz, Phys. Rev. B 4, 3460 (1971).
[23]J. D. Wiley, Solid State Commun. 8, 1865 (1970).
[24]The first-order calculation for $\lambda = 10.6$ μm and $T = 295$ °K, neglecting acoustical phonon scattering, gives a value of 18 MW/cm^2 for I_s.
[25]See, for example, A. Abragam, *The Principles of Nuclear Magnetism* (Clarendon, Oxford, England, 1961), p. 272ff.